Society For Biomaterials

Shotgun label-free proteomic analysis for identification of proteins in HaCaT human skin keratinocytes regulated by the administration of collagen from soft-shelled turtle

Tetsushi Yamamoto, Saori Nakanishi, Kuniko Mitamura, Atsushi Taga

Pathological and Biomolecule Analyses Laboratory, Faculty of Pharmacy, Kindai University, 3-4-1 Kowakae, Higashi-Osaka, Osaka 577-8502, Japan

Received 14 September 2017; accepted 13 October 2017
Published online 28 November 2017 in Wiley Online Library (wileyonlinelibrary.com). DOI: 10.1002/jbm.b.34034

Abstract: Soft-shelled turtles (*Pelodiscus sinensis*) are widely distributed in some Asian countries, and we previously reported that soft-shelled turtle tissue could be a useful material for collagen. In the present study, we performed shotgun liquid chromatography (LC)/mass spectrometry (MS)-based global proteomic analysis of collagen-administered human keratinocytes to examine the functional effects of collagen from soft-shelled turtle on human skin. Using a semiquantitative method based on spectral counting, we were able to successfully identify 187 proteins with expression levels that were changed more than twofold by the administration of collagen from soft-shelled turtle. Based on Gene Ontology analysis, the functions of these proteins closely correlated with cell–cell adhesion. In addition, epithelial–mesenchymal transition was induced by the administration of collagen from soft-shelled turtle through the down-regulation of E-cadherin expression. Moreover, collagen-administered keratinocytes significantly facilitated wound healing compared with nontreated cells in an *in vitro* scratch wound healing assay. These findings suggest that collagen from soft-shelled turtle provides significant benefits for skin wound healing and may be a useful material for pharmaceuticals and medical care products. © 2017 The Authors Journal of Biomedical Materials Research Part B: Applied Biomaterials Published by Wiley Periodicals, Inc. J Biomed Mater Res Part B: Appl Biomater 106B:2403–2413, 2018.

Key Words: collagen, soft-shelled turtle, E-cadherin, epithelial–mesenchymal transition, wound healing

How to cite this article: Yamamoto T, Nakanishi S, Mitamura K, Taga A 2018. Shotgun label-free proteomic analysis for identification of proteins in HaCaT human skin keratinocytes regulated by the administration of collagen from soft-shelled turtle. J Biomed Mater Res Part B 2018:106B:2403–2413.

INTRODUCTION

Collagen is a ubiquitous structural protein in both invertebrates and vertebrates, comprising >20 different types based on the function in each tissue.[1,2] These proteins are involved in the formation of fibrillar and microfibrillar networks of extracellular matrix and basement membranes to maintain the extracellular matrix environment.[3–7] Recent reports have demonstrated that collagen is able to interact with several cell surface receptors and regulate cell proliferation or apoptosis.[8,9] In addition, collagen is used for skin substitutes and drug delivery.[10–15] Therefore, collagen is an important material for cosmetics, pharmaceuticals, and medical care products.

Most of the collagen presently in use is derived from bovine and porcine skin. However, allergic reactions and connective tissue disorders, such as arthritis and lupus, have been reported with the use of collagen from these animals.[16] Moreover, these materials can potentially carry animal diseases, such as bovine spongiform encephalopathy and foot and mouth disease. Thus, these animals have been reconsidered as the main source for collagen products. In addition, many Muslims and Jews do not consume pig-derived food products, and many Hindus do not consume cow-derived products.[17] Therefore, collagen of marine origin, such as fish, sponges, and mollusks, was recently considered as a useful alternative to mammalian sources because of its high availability.[18–25] In addition, we previously reported that soft-shelled turtle (*Pelodiscus sinensis*) tissue could be a useful alternative for collagen.[26] Recently, several reports demonstrated its usefulness,[27,28] making collagen from soft-shelled turtle a useful material for cosmetics, pharmaceuticals, and medical care products.

However, collagen from soft-shelled turtle may differ greatly from that of mammalian resources in regards to physicochemical properties, amino acid compositions, and physiological functions due to the difference in the habitat environment. Therefore, further research is needed before using collagen from soft-shelled turtle as a source for collagen products. In the present study, we performed shotgun liquid chromatography (LC)/mass spectrometry (MS)-based

Correspondence to: A. Taga; e-mail: punk@phar.kindai.ac.jp
Contract grant sponsor: Grant-in-Aid for Scientific Research from the Japan Society for the Promotion of Science to T. Yamamoto; contract grant number: 15K09054

global proteomic analysis of collagen-administered human keratinocytes to examine the functional effects of collagen from soft-shelled turtle on human skin. We found that 187 proteins were differentially expressed in the collagen-administered keratinocytes compared with nontreated cells, and these proteins may be involved in wound healing in human skin.

MATERIALS AND METHODS

Chemicals

The chemicals used in this study were of the highest grade available and purchased from Wako Pure Chemical Industries (Osaka, Japan).

Turtles

Emperor tissue, a soft tissue in the region around the shell of soft-shelled turtles (*P. sinensis*), was provided by Shinuoei (Osaka, Japan).

Collagen extraction

Collagen extraction was performed in accordance with the our previous study.[26] Briefly, emperor tissue was treated with 0.1*M* formic acid at a ratio of 1:10 (w/v) for 24 h for demineralization. The sample was then treated with 0.1*M* sodium hydroxide (NaOH) at a ratio of 1:10 (w/v) for 3 days to remove noncollagenous proteins, including endogenous proteases. The NaOH solution was changed every day. Finally, the sample was incubated with 0.03*M* citric acid for 24 h. After incubation, the solution was centrifuged at 6500*g* for 20 min at 4°C and the supernatant collected as the collagen solution.

Cell culture

HaCaT immortalized human keratinocytes were purchased from CLS Cell Lines Service GmbH (Eppelheim, Germany). The cells were cultured in RPMI1640 medium supplemented with 10% fetal bovine serum (FBS) (Gibco, Carlsbad, CA, USA) in an atmosphere containing 5% CO_2.

Cell growth assay

Cells were plated at a density of 5×10^3 cells per well in a 96-well plate and grown in culture medium. The next day, the medium was changed and cells grown in collagen-containing culture medium. After 72 h, the cells were incubated with WST-8 cell counting reagent (Wako) and the optical density of the culture solution in the plate measured using an ELISA plate reader.

Protein preparation

HaCaT cells were plated in a 60-mm dish at a density of 2×10^5 cells per dish and grown in culture medium. The next day, the medium was changed and the cells grown in collagen-containing culture medium. After 72 h, the cells were solubilized in urea lysis buffer (7*M* urea, 2*M* thiourea, 5% CHAPS, 1% Triton X-100). The protein concentration was measured using the Bradford method.

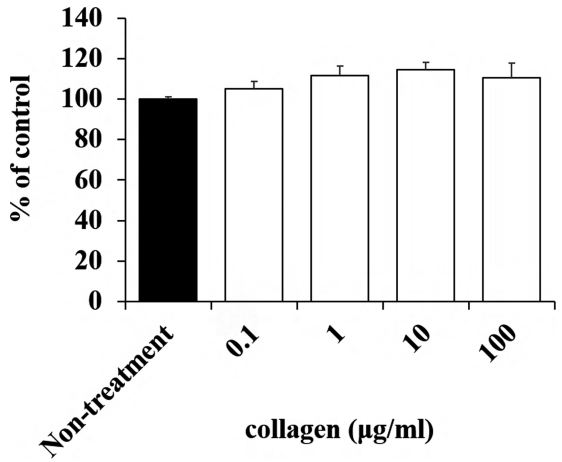

FIGURE 1. Cytotoxic effect of collagen administration in HaCaT cells. Suitable concentrations of collagen that are not cytotoxic to HaCaT cells were determined. No effect was observed on cell proliferation of HaCaT cells with collagen administration.

In-solution trypsin digestion

A gel-free digestion approach was performed in accordance a previously described protocol.[29] Briefly, 10 μg of protein extract from each sample was reduced by the addition of 45 m*M* dithiothreitol and 20 m*M* *tris*(2-carboxyethyl)phosphine, and then alkylated using 100 m*M* iodoacetic acid. After alkylation, the samples were digested with trypsin gold, mass spectrometry grade (Promega Corp., Madison, WI, USA) at 37°C for 24 h. Next, the digests were purified using PepClean C-18 Spin Columns (Thermo, Rockford, IL, USA) according to the manufacturer's protocol.

LC–MS/MS analysis for protein identification

Peptide samples (~2 μg) were injected into a peptide L-trap column (Chemicals Evaluation and Research Institute, Tokyo, Japan) using an HTC PAL autosampler (CTC Analytics, Zwingen, Switzerland) and further separated through a Paradigm MS4 (AMR, Tokyo, Japan) using a reverse-phase C18-column (L-column, 3 μm diameter gel particles and 120 Å pore size, 0.2 × 150 mm, Chemicals Evaluation and Research Institute). The mobile phase consisted of 0.1% formic acid in

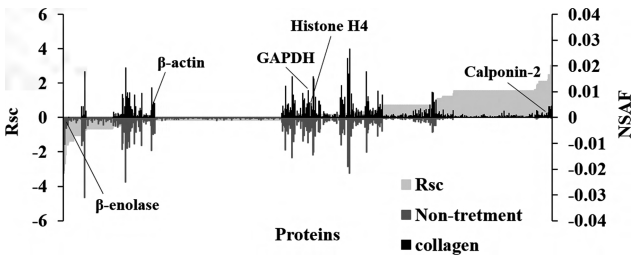

FIGURE 2. Semiquantitative comparison of identified proteins in collagen-administered and nontreated HaCaT cells. R_{sc} and normalized spectral abundance factor (NSAF) values calculated for identified proteins are on the *X*-axis. Protein expression is compared for collagen versus control. Proteins highly expressed in either collagen-administered cells or nontreated cells are near the right or left side of the X-axis. Housekeeping proteins are located around the center of the X-axis.

TABLE I. Differentially Expressed Proteins (>2-fold) Upon Administration of Collagen

No.	ID	Accession Number and Description		Number of Amino Acids	Fold Change (R_{sc})
1	H2B1K_HUMAN	O60814	Histone H2B type 1-K	126	−3.690
2	EF1A3_HUMAN	Q5VTE0	Putative elongation factor 1-alpha-like 3	462	−3.080
3	H2B1M_HUMAN	Q99879	Histone H2B type 1-M	126	−2.698
4	K2C3_HUMAN	P12035	Keratin, type II cytoskeletal 3	628	−2.178
5	H2A1H_HUMAN	Q96KK5	Histone H2A type 1-H	128	−1.611
6	RL10_HUMAN	P27635	60S ribosomal protein L10	214	−1.611
7	ARF3_HUMAN	P61204	ADP-ribosylation factor 3	181	−1.611
8	DYHC1_HUMAN	Q14204	Cytoplasmic dynein 1 heavy chain 1	4646	−1.477
9	TBAL3_HUMAN	A6NHL2	Tubulin alpha chain-like 3	446	−1.359
10	ENOB_HUMAN	P13929	Beta-enolase	434	−1.359
11	FLNB_HUMAN	O75369	Filamin-B	2602	−1.359
12	PDLI1_HUMAN	O00151	PDZ and LIM domain protein 1	329	−1.359
13	FLNA_HUMAN	P21333	Filamin-A	2647	−1.359
14	MYH14_HUMAN	Q7Z406	Myosin-14	1995	−1.359
15	K2C80_HUMAN	Q6KB66	Keratin, type II cytoskeletal 80	452	−1.359
16	K2C72_HUMAN	Q14CN4	Keratin, type II cytoskeletal 72	511	−1.053
17	POTEF_HUMAN	A5A3E0	POTE ankyrin domain family member F	1075	−1.053
18	GDIA_HUMAN	P31150	Rab GDP dissociation inhibitor alpha	447	−1.053
19	RS27A_HUMAN	P62979	Ubiquitin-40S ribosomal protein S27a	156	−1.053
20	CAH2_HUMAN	P00918	Carbonic anhydrase 2	260	−1.053
21	SEPT9_HUMAN	Q9UHD8	Septin-9	586	−1.053
22	PRP8_HUMAN	Q6P2Q9	Pre-mRNA-processing-splicing factor 8	2335	−1.053
23	IMB1_HUMAN	Q14974	Importin subunit beta-1	876	−1.053
24	HS105_HUMAN	Q92598	Heat shock protein 105 kDa	858	−1.053
25	PLST_HUMAN	P13797	Plastin-3	630	−1.053
26	H2A1D_HUMAN	P20671	Histone H2A type 1-D	130	−1.036
27	AL1A3_HUMAN	P47895	Aldehyde dehydrogenase family 1 member A3	512	1.020
28	HNRH1_HUMAN	P31943	Heterogeneous nuclear ribonucleoprotein H	449	1.102
29	PEPL_HUMAN	O60437	Periplakin	1756	1.102
30	LDHB_HUMAN	P07195	L-lactate dehydrogenase B chain	334	1.102
31	TPM4_HUMAN	P67936	Tropomyosin alpha-4 chain	248	1.102
32	2AAA_HUMAN	P30153	Serine/threonine-protein phosphatase 2A 65 kDa regulatory subunit A alpha isoform	589	1.102
33	EZRI_HUMAN	P15311	Ezrin	586	1.102
34	COR1C_HUMAN	Q9ULV4	Coronin-1C	474	1.102
35	SPTN1_HUMAN	Q13813	Spectrin alpha chain, nonerythrocytic 1	2472	1.182
36	H2AV_HUMAN	Q71UI9	Histone H2A.V	128	1.245
37	ARP3_HUMAN	P61158	Actin-related protein 3	418	1.245
38	TCPB_HUMAN	P78371	T-complex protein 1 subunit beta	535	1.245
39	AHSA1_HUMAN	O95433	Activator of 90 kDa heat shock protein ATPase homolog 1	338	1.245
40	KMT2A_HUMAN	Q03164	Histone-lysine *N*-methyltransferase 2A	3969	1.245
41	SYLC_HUMAN	Q9P2J5	Leucine-tRNA ligase, cytoplasmic	1176	1.245
42	PGAM1_HUMAN	P18669	Phosphoglycerate mutase 1	254	1.245
43	ICAL_HUMAN	P20810	Calpastatin	708	1.245
44	CISY_HUMAN	O75390	Citrate synthase, mitochondrial	466	1.245
45	LIMA1_HUMAN	Q9UHB6	LIM domain and actin-binding protein 1	759	1.245
46	CAPR1_HUMAN	Q14444	Caprin-1	709	1.245
47	MYADM_HUMAN	Q96S97	Myeloid-associated differentiation marker	322	1.245
48	PDCD4_HUMAN	Q53EL6	Programmed cell death protein 4	469	1.245
49	APEX1_HUMAN	P27695	DNA-(apurinic or apyrimidinic site) lyase	318	1.245
50	MARE1_HUMAN	Q15691	Microtubule-associated protein RP/EB family member 1	268	1.408
51	NACAM_HUMAN	E9PAV3	Nascent polypeptide-associated complex subunit alpha, muscle-specific form	2078	1.562
52	SHLB2_HUMAN	Q9NR46	Endophilin-B2	395	1.562
53	LIMS1_HUMAN	P48059	LIM and senescent cell antigen-like-containing domain protein 1	325	1.562
54	EHD1_HUMAN	Q9H4M9	EH domain-containing protein 1	534	1.562
55	TNPO1_HUMAN	Q92973	Transportin-1	898	1.562
56	PYGB_HUMAN	P11216	Glycogen phosphorylase, brain form	843	1.562
57	BZW1_HUMAN	Q7L1Q6	Basic leucine zipper and W2 domain-containing protein 1	419	1.562
58	AP2B1_HUMAN	P63010	AP-2 complex subunit beta	937	1.562

TABLE I. *Continued*

No.	ID	Accession Number and Description		Number of Amino Acids	Fold Change (R_{sc})
59	CMC1_HUMAN	O75746	Calcium-binding mitochondrial carrier protein Aralar1	678	1.562
60	SKAP_HUMAN	Q9Y448	Small kinetochore-associated protein	316	1.562
61	CD9_HUMAN	P21926	CD9 antigen	228	1.562
62	P4HA1_HUMAN	P13674	Prolyl 4-hydroxylase subunit alpha-1	534	1.562
63	PPAC_HUMAN	P24666	Low molecular weight phosphotyrosine protein phosphatase	158	1.562
64	FUBP2_HUMAN	Q92945	Far upstream element-binding protein 2	711	1.562
65	RGPD2_HUMAN	P0DJD1	RANBP2-like and GRIP domain-containing protein 2	1756	1.562
66	RAB1C_HUMAN	Q92928	Putative Ras-related protein Rab-1C	201	1.562
67	HUWE1_HUMAN	Q7Z6Z7	E3 ubiquitin-protein ligase HUWE1	4374	1.562
68	IPYR2_HUMAN	Q9H2U2	Inorganic pyrophosphatase 2, mitochondrial	334	1.562
69	CERS2_HUMAN	Q96G23	Ceramide synthase 2	380	1.562
70	IRS4_HUMAN	O14654	Insulin receptor substrate 4	1257	1.562
71	DDX3X_HUMAN	O00571	ATP-dependent RNA helicase DDX3X	662	1.562
72	PARP1_HUMAN	P09874	Poly[ADP-ribose] polymerase 1	1014	1.562
73	MAP4_HUMAN	P27816	Microtubule-associated protein 4	1152	1.562
74	LAT1_HUMAN	Q01650	Large neutral amino acids transporter small subunit 1	507	1.562
75	CARD6_HUMAN	Q9BX69	Caspase recruitment domain-containing protein 6	1037	1.562
76	PCD16_HUMAN	Q96JQ0	Protocadherin-16	3298	1.562
77	CP250_HUMAN	Q9BV73	Centrosome-associated protein CEP250	2442	1.562
78	MCM3_HUMAN	P25205	DNA replication licensing factor MCM3	808	1.562
79	SYSC_HUMAN	P49591	Serine-tRNA ligase, cytoplasmic	514	1.562
80	EPHA4_HUMAN	P54764	Ephrin type-A receptor 4	986	1.562
81	NT5D1_HUMAN	Q5TFE4	5-nucleotidase domain-containing protein 1	455	1.562
82	GIPC3_HUMAN	Q8TF64	PDZ domain-containing protein GIPC3	312	1.562
83	MXRA5_HUMAN	Q9NR99	Matrix-remodeling-associated protein 5	2828	1.562
84	CO4A4_HUMAN	P53420	Collagen alpha-4 (IV) chain	1690	1.562
85	POTEB_HUMAN	Q6S5H4	POTE ankyrin domain family member B	581	1.562
86	MYH1_HUMAN	P12882	Myosin-1	1939	1.562
87	NFRKB_HUMAN	Q6P4R8	Nuclear factor related to kappa-B-binding protein	1299	1.562
88	NAC2_HUMAN	Q9UPR5	Sodium/calcium exchanger 2	921	1.562
89	NRK2_HUMAN	Q9NPI5	Nicotinamide riboside kinase 2	230	1.562
90	BRM1L_HUMAN	Q5PSV4	Breast cancer metastasis-suppressor 1-like protein	323	1.562
91	SAP3_HUMAN	P17900	Ganglioside GM2 activator	193	1.562
92	APBA1_HUMAN	Q02410	Amyloid beta A4 precursor protein-binding family A member 1	837	1.562
93	RS14_HUMAN	P62263	40S ribosomal protein S14	151	1.562
94	ENDOV_HUMAN	Q8N8Q3	Endonuclease V	282	1.562
95	UBE4B_HUMAN	O95155	Ubiquitin conjugation factor E4 B	1302	1.562
96	F134C_HUMAN	Q86VR2	Protein FAM134C	466	1.562
97	ACSM5_HUMAN	Q6NUN0	Acyl-coenzyme A synthetase ACSM5, mitochondrial	579	1.562
98	DPOE1_HUMAN	Q07864	DNA polymerase epsilon catalytic subunit A	2286	1.562
99	SRRT_HUMAN	Q9BXP5	Serrate RNA effector molecule homolog	876	1.562
100	EXOC1_HUMAN	Q9NV70	Exocyst complex component 1	894	1.562
101	GDE1_HUMAN	Q9NZC3	Glycerophosphodiester phosphodiesterase 1	331	1.562
102	CAMP3_HUMAN	Q9P1Y5	Calmodulin-regulated spectrin-associated protein 3	1249	1.562
103	BCAS3_HUMAN	Q9H6U6	Breast carcinoma-amplified sequence 3	928	1.562
104	NXF2_HUMAN	Q9GZY0	Nuclear RNA export factor 2	626	1.562
105	HIC1_HUMAN	Q14526	Hypermethylated in cancer 1 protein	733	1.562
106	VP13C_HUMAN	Q709C8	Vacuolar protein sorting-associated protein 13C	3753	1.562
107	DCE1_HUMAN	Q99259	Glutamate decarboxylase 1	594	1.562
108	RUVB2_HUMAN	Q9Y230	RuvB-like 2	463	1.562
109	UBA1_HUMAN	P22314	Ubiquitin-like modifier-activating enzyme 1	1058	1.562
110	ANX11_HUMAN	P50995	Annexin A11	505	1.562
111	2AAB_HUMAN	P30154	Serine/threonine-protein phosphatase 2A 65 kDa regulatory subunit A beta isoform	601	1.562
112	TFG_HUMAN	Q92734	Protein TFG	400	1.562
113	1433Z_HUMAN	P63104	14-3-3 protein zeta/delta	245	1.562
114	C1TC_HUMAN	P11586	C-1-tetrahydrofolate synthase, cytoplasmic	935	1.562
115	PRDX4_HUMAN	Q13162	Peroxiredoxin-4	271	1.562
116	TENA_HUMAN	P24821	Tenascin	2201	1.562

TABLE I. *Continued*

No.	ID	Accession Number and Description		Number of Amino Acids	Fold Change (R_{sc})
117	MIF_HUMAN	P14174	Macrophage migration inhibitory factor	115	1.562
118	NIPS2_HUMAN	O75323	Protein NipSnap homolog 2	286	1.562
119	CTNB1_HUMAN	P35222	Catenin beta-1	781	1.562
120	ADIRF_HUMAN	Q15847	Adipogenesis regulatory factor	76	1.562
121	COASY_HUMAN	Q13057	Bifunctional coenzyme A synthase	564	1.562
122	TF_HUMAN	P13726	Tissue factor	295	1.562
123	MATR3_HUMAN	P43243	Matrin-3	847	1.562
124	RAB4A_HUMAN	P20338	Ras-related protein Rab-4A	218	1.562
125	IF4H_HUMAN	Q15056	Eukaryotic translation initiation factor 4H	248	1.562
126	ERP29_HUMAN	P30040	Endoplasmic reticulum resident protein 29	261	1.562
127	RL30_HUMAN	P62888	60S ribosomal protein L30	115	1.562
128	PPCE_HUMAN	P48147	Prolyl endopeptidase	710	1.562
129	UBFL1_HUMAN	P0CB47	Putative upstream-binding factor 1-like protein 1	393	1.562
130	HGB1A_HUMAN	B2RPK0	Putative high mobility group protein B1-like 1	211	1.562
131	TM163_HUMAN	Q8TC26	Transmembrane protein 163	289	1.562
132	DCK_HUMAN	P27707	Deoxycytidine kinase	260	1.562
133	PSB6_HUMAN	P28072	Proteasome subunit beta type-6	239	1.562
134	GLYC_HUMAN	P34896	Serine hydroxymethyltransferase, cytosolic	483	1.562
135	ETFB_HUMAN	P38117	Electron transfer flavoprotein subunit beta	255	1.562
136	SEPT2_HUMAN	Q15019	Septin-2	361	1.562
137	IG2AS_HUMAN	Q6U949	Putative insulin-like growth factor 2 antisense gene protein	168	1.562
138	SYEP_HUMAN	P07814	Bifunctional glutamate/proline-tRNA ligase	1512	1.562
139	GGH_HUMAN	Q92820	Gamma-glutamyl hydrolase	318	1.562
140	SMC5_HUMAN	Q8IY18	Structural maintenance of chromosomes protein 5	1101	1.562
141	3BHS2_HUMAN	P26439	3 beta-hydroxysteroid dehydrogenase/Delta 5–>4-isomerase type 2	372	1.562
142	SIAS_HUMAN	Q9NR45	Sialic acid synthase	359	1.562
143	DYH7_HUMAN	Q8WXX0	Dynein heavy chain 7, axonemal	4024	1.562
144	GRM2_HUMAN	Q14416	Metabotropic glutamate receptor 2	872	1.562
145	PLCB_HUMAN	O15120	1-acyl-sn-glycerol-3-phosphate acyltransferase beta	278	1.562
146	PNPO_HUMAN	Q9NVS9	Pyridoxine-5-phosphate oxidase	261	1.562
147	GFPT1_HUMAN	Q06210	Glutamine-fructose-6-phosphate aminotransferase [isomerizing] 1	699	1.562
148	INADL_HUMAN	Q8NI35	InaD-like protein	1801	1.562
149	CPMD8_HUMAN	Q8IZJ3	C3 and PZP-like alpha-2-macroglobulin domain-containing protein 8	1885	1.562
150	CO9A1_HUMAN	P20849	Collagen alpha-1(IX) chain	921	1.562
151	DNJA2_HUMAN	O60884	DnaJ homolog subfamily A member 2	412	1.562
152	GASP1_HUMAN	Q5JY77	G-protein coupled receptor-associated sorting protein 1	1395	1.562
153	BIRC3_HUMAN	Q13489	Baculoviral IAP repeat-containing protein 3	604	1.562
154	IL2RG_HUMAN	P31785	Cytokine receptor common subunit gamma	369	1.562
155	FUCM_HUMAN	A2VDF0	Fucose mutarotase	154	1.562
156	KAD3_HUMAN	Q9UIJ7	GTP:AMP phosphotransferase AK3, mitochondrial	227	1.562
157	GSX2_HUMAN	Q9BZM3	GS homeobox 2	304	1.562
158	MIMIT_HUMAN	Q8N183	Mimitin, mitochondrial	169	1.562
159	CYC_HUMAN	P99999	Cytochrome *c*	105	1.562
160	CC141_HUMAN	Q6ZP82	Coiled-coil domain-containing protein 141	1450	1.562
161	ZN503_HUMAN	Q96F45	Zinc finger protein 503	646	1.562
162	CHD7_HUMAN	Q9P2D1	Chromodomain helicase DNA binding protein 7	2997	1.562
163	RADI_HUMAN	P35241	Radixin	583	1.633
164	CAN1_HUMAN	P07384	Calpain-1 catalytic subunit	714	1.633
165	CATB_HUMAN	P07858	Cathepsin B	339	1.660
166	EF1G_HUMAN	P26641	Elongation factor 1-gamma	437	1.875
167	CNN2_HUMAN	Q99439	Calponin-2	309	1.938
168	GELS_HUMAN	P06396	Gelsolin	782	1.938
169	KRT81_HUMAN	Q14533	Keratin, type II cuticular Hb1	505	2.094
170	EIF3E_HUMAN	P60228	Eukaryotic translation initiation factor 3 subunit E	445	2.094
171	DAZP1_HUMAN	Q96EP5	DAZ-associated protein 1	407	2.094
172	SURF4_HUMAN	O15260	Surfeit locus protein 4	269	2.094

TABLE I. *Continued*

No.	ID	Accession Number and Description		Number of Amino Acids	Fold Change (R_{sc})
173	GGCT_HUMAN	O75223	Gamma-glutamylcyclotransferase	188	2.094
174	HNRH2_HUMAN	P55795	Heterogeneous nuclear ribonucleoprotein H2	449	2.094
175	AT1A1_HUMAN	P05023	Sodium/potassium-transporting ATPase subunit alpha-1	1023	2.094
176	OLA1_HUMAN	Q9NTK5	Obg-like ATPase 1	396	2.094
177	RL1D1_HUMAN	O76021	Ribosomal L1 domain-containing protein 1	490	2.094
178	IF4A3_HUMAN	P38919	Eukaryotic initiation factor 4A-III	411	2.094
179	MESD_HUMAN	Q14696	LDLR chaperone MESD	234	2.094
180	K1C27_HUMAN	Q7Z3Y8	Keratin, type I cytoskeletal 27	459	2.094
181	CNDP2_HUMAN	Q96KP4	Cytosolic nonspecific dipeptidase	475	2.191
182	H2A2A_HUMAN	Q6FI13	Histone H2A type 2-A	130	2.481
183	PYGL_HUMAN	P06737	Glycogen phosphorylase, liver form	847	2.481
184	H2A1C_HUMAN	Q93077	Histone H2A type 1-C	130	2.481
185	ADT1_HUMAN	P12235	ADP/ATP translocase 1	298	3.039
186	VPP4_HUMAN	Q9HBG4	V-type proton ATPase 116 kDa subunit a isoform 4	840	3.049
187	H2B1H_HUMAN	Q93079	Histone H2B type 1-H	126	4.672

water as solution A and acetonitrile as solution B. The column flow rate was 1 μL/min with a concentration gradient of 5% B to 40% B over 120 min. Gradient-eluted peptides were analyzed using an LTQ ion-trap mass spectrometer (Thermo). The results were acquired in a data-dependent manner in which MS/MS fragmentation was performed on the two most intense peaks of every full MS scan.

All MS/MS spectral data were searched against the SwissProt *Homo Sapiens* database using Mascot (version 2.4.01, Matrix Science, London, UK). The search criteria were set as follows: enzyme, trypsin; allowance of up to two missed cleavage peptides; mass tolerance ±2.0 Da and MS/MS tolerance ±0.8 Da; and modifications of cysteine carbamidomethylation and methionine oxidation.

Semiquantitative analysis of identified proteins

The fold changes in expressed proteins on a base 2 logarithmic scale were calculated using the Rsc based on spectral counting.[30] Relative amounts of identified proteins were calculated using the normalized spectral abundance factor (NSAF).[31] Differentially expressed proteins were chosen so that their *R*sc was >1 or ≤ 1, which correspond to fold changes of >2 or <0.5.

Bioinformatics

Functional annotations for proteins identified to be regulated by collagen administration were processed using the Database for Annotation, Visualization, and Integrated Discovery (DAVID) version 6.8 (http://david.abcc.ncifcrf.gov/home.jsp).[32–34]

Western blot analysis

A total of 5 μg of cell extract was added to each well and subjected to SDS-PAGE under reducing conditions. The separated proteins were transferred to polyvinylidene fluoride transfer membranes. Following blocking in TBS–Tween-20 (0.1%) buffer with 5% skim milk for 2 h at room temperature, the membranes were incubated at 4°C overnight with an anti-E-cadherin antibody (1:5,000; Cell Signaling Technology, Beverly, MA), antivimentin antibody (1:1000; Cell Signaling Technology), or antisnail antibody (1:1000; Cell Signaling Technology). Next, the membranes were washed and incubated with HRP-conjugated antirabbit IgG antibody (American Qualex, San Clemente, CA). Following washing, the blots were visualized using SuperSignal West Dura Extended Duration substrate (Thermo Fisher Scientific) and bands detected using the myECL Imager system (version 2.0; Thermo Fisher Scientific). Next, the same membranes were reprobed with an anti-β-actin antibody (Santa Cruz Biotechnology, Dallas, TX) to confirm equal loading of the proteins. All Western blot analyses were performed in triplicate.

Scratch assay

Cells were plated in 35 mm dishes (5×10^5 cells/dish) and incubated for 24 h at 37°C in a humidified 5% CO_2 atmosphere to assure confluency. The center of the monolayer was scratched by scraping the cells with a sterile 200-μL pipette tip.[35] After scratching, the dish was gently washed with PBS to remove the detached cells and the medium changed in collagen-containing culture medium. A microscope system was used to take photographs from the scratch area 0 and 8 h after scratching (Olympus, Tokyo, Japan).

Statistical analysis

All data are presented as the mean ± standard error of the mean. The data were analyzed using one-way analysis of variance followed by Dunnett's test or the unpaired *t* test. $P < 0.01$ was considered significant in all analyses. Computations were performed in GraphPad Prism version 5.1 (GraphPad Software, La Jolla, CA, USA).

RESULTS

Cytotoxicity of collagen against HaCaT cells

To examine the cytotoxic effect of collagen on HaCaT cells, we assessed the cell growth rate when cells were grown in culture medium containing the collagen solution at a concentration of 0.1–100 μg/mL. The growth rate of HaCaT cells cultured in the medium containing collagen was not

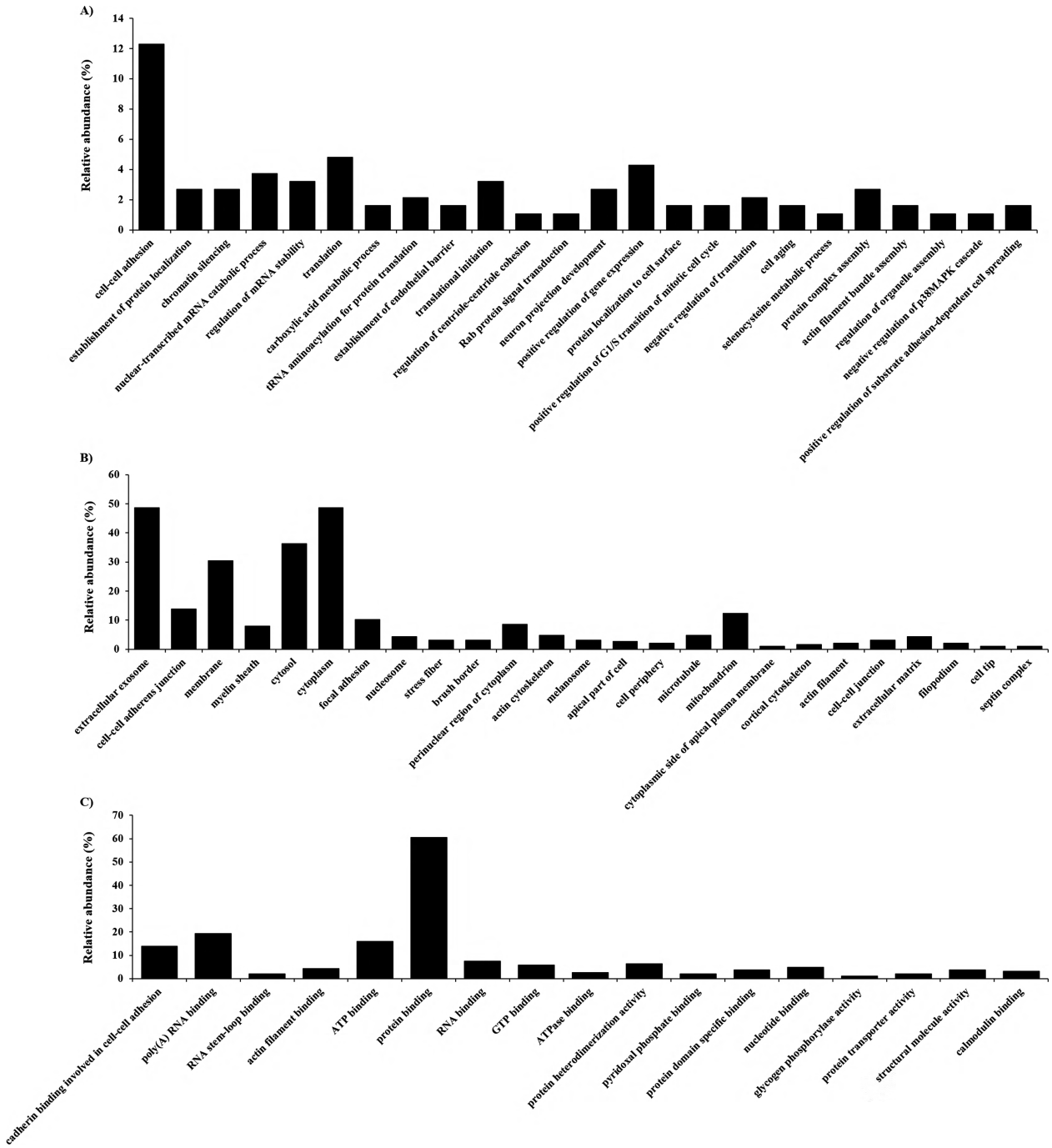

FIGURE 3. Gene ontology (GO) analysis for identified proteins. (A) Proteins assigned to biological process, (B) cellular component, and (C) molecular function GO term categories. Only significant categories ($p < 0.05$) are shown.

inhibited at 72 h compared with nontreated cells (Fig. 1). Therefore, we used 100 μg/mL collagen in the following experiments.

Protein identification and semiquantitative comparison of identified proteins in collagen-administered HaCaT cells

To investigate the effect of collagen on the cells in the basal layer of the skin, we determined the molecular profile of proteins in HaCaT cells whose expression levels were regulated by collagen using shotgun proteomics. We performed a label-free semiquantitative method based on spectral counting to determine the proteins whose expression levels were regulated by collagen. In Figure 2, each R_{sc} value is plotted against the corresponding protein (X-axis) in increasing order from left to right for proteins identified in collagen-administered HaCaT cells (collagen) and nontreated cells (nontreatment). A positive value indicates increased

TABLE II. Differentially Expressed Proteins Categorized as Cadherin Binding Involved in Cell–Cell Adhesion Proteins in Gene Ontology

No.	Accession Number and Description		Fold Change (R_{sc})
1	O00151	PDZ and LIM domain protein 1	−1.359
2	P21333	Filamin-A	−1.359
3	O75369	Filamin-B	−1.359
4	Q9UHD8	Septin-9	−1.053
5	P15311	Ezrin	1.102
6	O60437	Periplakin	1.102
7	Q13813	Spectrin alpha chain, nonerythrocytic 1	1.182
8	Q9UHB6	LIM domain and actin-binding protein 1	1.245
9	O95433	Activator of 90 kDa heat shock protein ATPase homolog 1	1.245
10	P20810	Calpastatin	1.245
11	Q15691	Microtubule-associated protein RP/EB family member 1	1.408
12	Q7L1Q6	Basic leucine zipper and W2 domain-containing protein 1	1.562
13	Q9NR46	Endophilin-B2	1.562
14	O00571	ATP-dependent RNA helicase DDX3X	1.562
15	P35222	Catenin beta-1	1.562
16	Q9H4M9	EH domain-containing protein 1	1.562
17	Q15056	Eukaryotic translation initiation factor 4H	1.562
18	P63104	14-3-3 protein zeta/delta	1.562
19	Q15019	Septin-2	1.562
20	P28072	Proteasome subunit beta type-6	1.562
21	P35241	Radixin	1.633
22	P26641	Elongation factor 1-gamma	1.875
23	Q99439	Calponin-2	1.938
24	P60228	Eukaryotic translation initiation factor 3 subunit E	2.094
25	Q9NTK5	Obg-like ATPase 1	2.094
26	O76021	Ribosomal L1 domain-containing protein 1	2.094

expression in the collagen-treated cells and a negative value decreased expression in the collagen-treated cells. The NSAF value (Fig. 2, bar) was also plotted on the X-axis for each corresponding protein with collagen treatment above the X-axis and control below. Proteins with a high positive or negative R_{sc} value would be candidates for proteins regulated by collagen.

As a result of semiquantification, a total of 187 differentially expressed proteins were identified (Table I). The expression levels of housekeeping proteins β-actin, GAPDH, and histone H4 were not changed by collagen administration.

Functional annotation of proteins regulated by collagen

Gene ontology (GO) analysis was performed with the candidate proteins for each biological process [Fig. 3(A)], cellular component [Fig. 3(B)], and molecular function [Fig. 3(C)] using DAVID. Some of the differentially expressed proteins were related to cell adhesion, and we focused on the function of proteins classified as cadherin binding involved in cell–cell adhesion (Table II).

Effect of collagen administration on the expression level of E-cadherin and EMT marker proteins in HaCaT cells

To investigate whether collagen administration affected the level of cadherin expression, we examined the expression of E-cadherin in collagen-administered HaCaT cells. The expression of E-cadherin clearly decreased with collagen administration compared with nontreated cells (Fig. 4). Next, we examined the expression levels of vimentin and snail to investigate whether epithelial–mesenchymal transition (EMT) was induced in correlation with the downregulation of E-cadherin. The expression of vimentin and snail clearly increased with collagen administration compared with nontreated cells (Fig. 4).

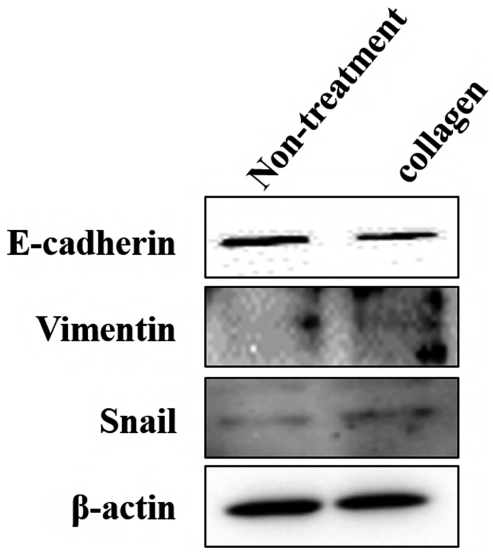

FIGURE 4. Expression levels of E-cadherin and EMT markers in HaCaT cells. E-cadherin expression was decreased with the administration of collagen, whereas the expression levels of vimentin and snail were increased by the administration of collagen compared with nontreated cells.

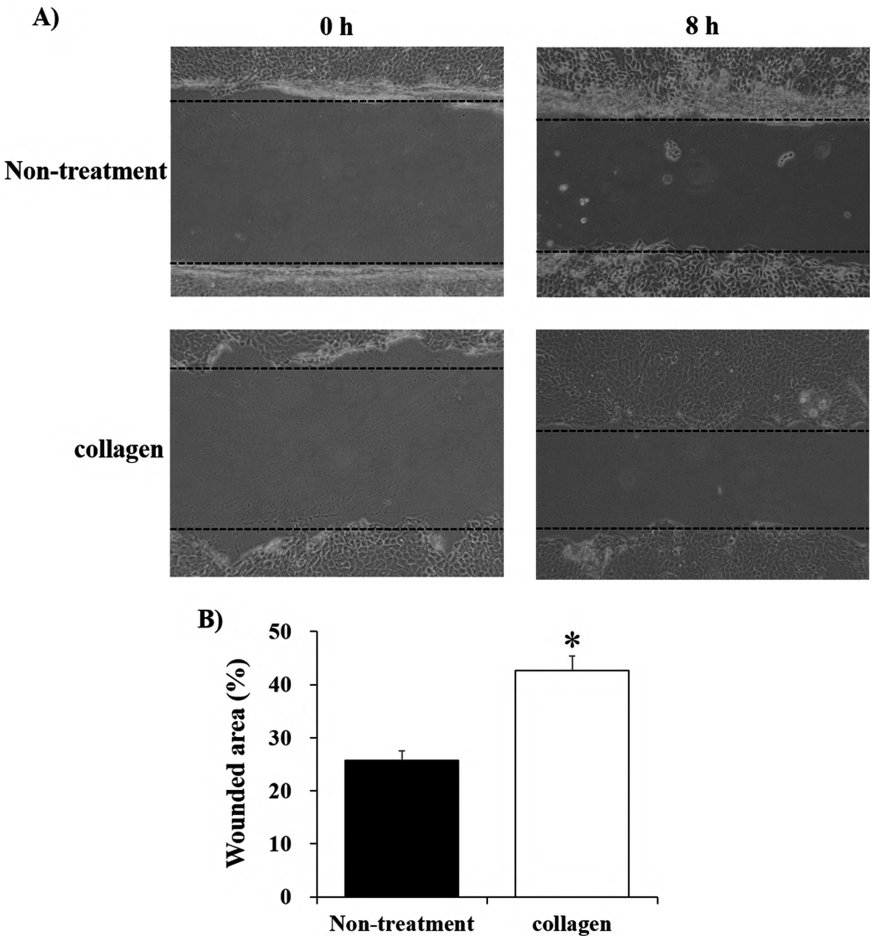

FIGURE 5. Wound healing assay. (A) Microscopic images of wound healing over 8 h. (B) The percentage of wounded area in collagen-administered HaCaT cells was significantly larger than in nontreated cells. $*p < 0.01$.

Effect of collagen administration on keratinocyte migration in a scratch-wound healing process

To investigate whether EMT affected the migration capability of HaCaT cells, we performed an *in vitro* wound healing study using the HaCaT scratch model. Photographs were taken before treatment and after 8 h of incubation at 37°C in 5% CO_2 [Fig. 5(A)]. Collagen-administered cells significantly facilitated wound healing compared with nontreated cells [Fig. 5(B)].

DISCUSSION

In this study, we used a gel-free LC–MS-based proteomics approach to examine the functional effects of collagen from soft-shelled turtle on human skin. Although spectral counting may not accurately reflect the quantity information,[36] it is useful and has been used in many studies, including those searching for novel diagnostic biomarkers.[37–42] We were able to successfully identify several proteins whose expression levels were changed >2-fold in HaCaT cells by the administration of collagen using a semiquantitative method based on spectral counting.

To examine the role of these identified proteins, we performed GO analysis. The functional category that directly relates to cell–cell adhesion was obtained from among the GO terms on molecular function, biological process, and cellular component. We focused on the functions of proteins classified as cadherin binding involved in cell–cell adhesion because they play important roles in cadherin-mediated cell adhesion; thus, changes in the expression levels of these proteins with the administration of collagen from soft-shelled turtle may affect the expression of cadherin. To evaluate this hypothesis, we examined the expression of a major cadherin protein in epithelial cells, E-cadherin; its expression level was decreased with the administration of collagen from soft-shelled turtle. As down-regulation of E-cadherin is an important factor in EMT induction, we examined the expression of EMT markers in HaCaT cells to investigate whether EMT was induced in keratinocytes by the administration of collagen. The increase in expression of vimentin, a mesenchymal marker,[43] and snail, a major inducer of EMT via suppression of E-cadherin expression,[43,44] in collagen-administered HaCaT cells compared with nontreated cells suggests that the administration of collagen from soft-shelled turtle induces EMT in human keratinocytes. Recent studies reported that human collagen type I can induce EMT in some cell types,[45–48] and collagen from soft-shelled turtle as used in this study may have a similar effect.

EMT was originally described as a phenomenon observed during gastrulation in the early embryo.[49] Recently, EMT was considered to be associates with tissue repair responses to injuries in parenchymal organs, including skin.[43,50] Therefore, we performed an *in vitro* wound healing assay using a cell scratch model to clarify the effect of EMT of HaCaT cells induced by the administration of collagen from soft-shelled turtle on the wound healing process. The significant promotion of wound healing in HaCaT cells administered collagen suggests that administration of collagen from soft-shelled turtle enhances the wound healing ability of keratinocytes through the induction of EMT. However, the mechanism of the induction of EMT of keratinocytes upon administration of collagen from soft-shelled turtle is unclear. In this study, we focused on the function of proteins listed in Table II, in which the expression level of β-catenin was increased with collagen administration. A previous report demonstrated that overexpression of β-catenin induced cell migration and invasion through the induction of EMT via up-regulation of mesenchymal markers, including vimentin, and down-regulation of epithelial markers, including E-cadherin.[51] Therefore, increased expression of β-catenin may be one of the mechanisms underlying the induction of EMT after the administration of collagen from soft-shelled turtle. Further studies are necessary to clarify the mechanism of increased β-catenin expression and the other mechanisms for EMT induction.

In conclusion, we measured the changes in protein expression in HaCaT cells administered collagen from soft-shelled turtle using a shotgun LC/MS-based global proteomic analysis and found that the administration of collagen induced the EMT of keratinocytes and facilitated wound healing. Therefore, collagen from soft-shelled turtle may provide significant benefits for skin wound healing and be a useful material for pharmaceuticals and medical care products.

ACKNOWLEDGMENTS

We are grateful to Mr. T. Aboshi for providing the soft-shelled turtles used in the study (Shin-uoei, Inc.).

REFERENCES

1. Gelse K, Poschl E, Aigner T. Collagens–structure, function, and biosynthesis. Adv Drug Deliv Rev 2003;55(12):1531–1546.
2. Myllyharju J, Kivirikko KI. Collagens, modifying enzymes and their mutations in humans, flies and worms. Trends Genet 2004;20(1): 33–43.
3. Birk DE, Trelstad RL. Extracellular compartments in tendon morphogenesis: Collagen fibril, bundle, and macroaggregate formation. J Cell Biol 1986;103(1):231–240.
4. Adachi E, Hayashi T. Anchoring of epithelia to underlying connective tissue: Evidence of frayed ends of collagen fibrils directly merging with meshwork of lamina densa. J Electron Microsc (Tokyo) 1994;43(5):264–271.
5. Park KH, Bae YH. Phenotype of hepatocyte spheroids in Arg-GLY-Asp (RGD) containing a thermo-reversible extracellular matrix. Biosci Biotechnol Biochem 2002;66(7):1473–1478.
6. Liu B, Weinzimer SA, Gibson TB, Mascarenhas D, Cohen P. Type I alpha collagen is an IGFBP-3 binding protein. Growth Horm IGF Res 2003;13(2–3):89–97.
7. Di Lullo GA, Sweeney SM, Korkko J, Ala-Kokko L, San Antonio JD. Mapping the ligand-binding sites and disease-associated mutations on the most abundant protein in the human, type I collagen. J Biol Chem 2002;277(6):4223–4231.
8. Saby C, Buache E, Brassart-Pasco S, El Btaouri H, Courageot MP, Van Gulick L, Garnotel R, Jeannesson P, Morjani H. Type I collagen aging impairs discoidin domain receptor 2-mediated tumor cell growth suppression. Oncotarget 2016;7(18):24908–24927.
9. Maquoi E, Assent D, Detilleux J, Pequeux C, Foidart JM, Noel A. MT1-MMP protects breast carcinoma cells against type I collagen-induced apoptosis. Oncogene 2012;31(4):480–493.
10. Gorell ES, Leung TH, Khuu P, Lane AT. Purified type I collagen wound matrix improves chronic wound healing in patients with recessive dystrophic epidermolysis bullosa. Pediatr Dermatol 2015;32(2):220–225.
11. Shevchenko RV, Sibbons PD, Sharpe JR, James SE. Use of a novel porcine collagen paste as a dermal substitute in full-thickness wounds. Wound Repair Regen 2008;16(2):198–207.
12. Wollina U, Meseg A, Weber A. Use of a collagen-elastin matrix for hard to treat soft tissue defects. Int Wound J 2011;8(3):291–296.
13. Barhoumi A, Salvador-Culla B, Kohane DS. NIR-triggered drug delivery by collagen-mediated second harmonic generation. Adv Healthc Mater 2015.
14. Wallace DG, Rosenblatt J. Collagen gel systems for sustained delivery and tissue engineering. Adv Drug Deliv Rev 2003;55(12): 1631–1649.
15. Friess W. Collagen–biomaterial for drug delivery. Eur J Pharm Biopharm 1998;45(2):113–136.
16. Lynn AK, Yannas IV, Bonfield W. Antigenicity and immunogenicity of collagen. J Biomed Mater Res B Appl Biomater 2004;71(2): 343–354.
17. Pranoto Y, Lee CM, Park HJ. Characterizations of fish gelatin films added with gellan and kappa-carrageenan. LWT Food Sci Technol 2007;40(5):766–774.
18. Muralidharan N, Jeya Shakila R, Sukumar D, Jeyasekaran G. Skin, bone and muscle collagen extraction from the trash fish, leather jacket (*Odonus niger*) and their characterization. J Food Sci Technol 2013;50(6):1106–1113.
19. Wang Y, Regenstein JM. Effect of EDTA, HCl, and citric acid on Ca salt removal from Asian (silver) carp scales prior to gelatin extraction. J Food Sci 2009;74(6):C426–C431.
20. Wang C, Zhan CL, Cai QF, Du CH, Liu GM, Su WJ, Cao MJ. Expression and characterization of common carp (*Cyprinus carpio*) matrix metalloproteinase-2 and its activity against type I collagen. J Biotechnol 2014;177:45–52.
21. Benjakul S, Thiansilakul Y, Visessanguan W, Roytrakul S, Kishimura H, Prodpran T, Meesane J. Extraction and characterisation of pepsin-solubilised collagens from the skin of bigeye snapper (*Priacanthus tayenus* and *Priacanthus macracanthus*). J Sci Food Agric 2010;90(1):132–138.
22. Nalinanon S, Benjakul S, Kishimura H. Collagens from the skin of arabesque greenling (*Pleurogrammus azonus*) solubilized with the aid of acetic acid and pepsin from albacore tuna (*Thunnus alalunga*) stomach. J Sci Food Agric 2010;90(9):1492–1500.
23. Tziveleka LA, Ioannou E, Tsiourvas D, Berillis P, Foufa E, Roussis V. Collagen from the Marine sponges *Axinella cannabina* and *Suberites carnosus*: Isolation and morphological, biochemical, and biophysical characterization. Mar Drugs 2017;15(6).
24. Pallela R, Venkatesan J, Janapala VR, Kim SK. Biophysicochemical evaluation of chitosan-hydroxyapatite-marine sponge collagen composite for bone tissue engineering. J Biomed Mater Res A 2012;100(2):486–495.
25. Coelho RCG, Marques ALP, Oliveira SM, Diogo GS, Pirraco RP, Moreira-Silva J, Xavier JC, Reis RL, Silva TH, Mano JF. Extraction and characterization of collagen from Antarctic and Sub-Antarctic squid and its potential application in hybrid scaffolds for tissue engineering. Mater Sci Eng C Mater Biol Appl 2017;78:787–795.
26. Yamamoto T, Uemura K, Sawashi Y, Mitamura K, Taga A. Optimization of method to extract collagen from "emperor" tissue of soft-shelled turtles. J Oleo Sci 2016;65(2):169–175.
27. Zou Y, Wang L, Cai P, Li P, Zhang M, Sun Z, Sun C, Xu W, Wang D. Effect of ultrasound assisted extraction on the physicochemical and functional properties of collagen from soft-shelled turtle calipash. Int J Biol Macromol 2017.

28. Yang Y, Li C, Song W, Wang W, Qian G. Purification, optimization and physicochemical properties of collagen from soft-shelled turtle calipash. Int J Biol Macromol 2016;89:344–352.
29. Bluemlein K, Ralser M. Monitoring protein expression in whole-cell extracts by targeted label- and standard-free LC–MS/MS. Nat Protoc 2011;6(6):859–869.
30. Old WM, Meyer-Arendt K, Aveline-Wolf L, Pierce KG, Mendoza A, Sevinsky JR, Resing KA, Ahn NG. Comparison of label-free methods for quantifying human proteins by shotgun proteomics. Mol Cell Proteomics 2005;4(10):1487–1502.
31. Zybailov B, Coleman MK, Florens L, Washburn MP. Correlation of relative abundance ratios derived from peptide ion chromatograms and spectrum counting for quantitative proteomic analysis using stable isotope labeling. Anal Chem 2005;77(19):6218–6224.
32. Dennis G, Jr., Sherman BT, Hosack DA, Yang J, Gao W, Lane HC, Lempicki RA. DAVID: Database for annotation, visualization, and integrated discovery. Genome Biol 2003;4(5):P3.
33. Huang da W, Sherman BT, Lempicki RA. Systematic and integrative analysis of large gene lists using DAVID bioinformatics resources. Nat Protoc 2009;4(1):44–57.
34. Huang da W, Sherman BT, Lempicki RA. Bioinformatics enrichment tools: Paths toward the comprehensive functional analysis of large gene lists. Nucleic Acids Res 2009;37(1):1–13.
35. Liang CC, Park AY, Guan JL. *In vitro* scratch assay: A convenient and inexpensive method for analysis of cell migration *in vitro*. Nat Protoc 2007;2(2):329–333.
36. Lundgren DH, Hwang SI, Wu L, Han DK. Role of spectral counting in quantitative proteomics. Expert Rev Proteomics 2010;7(1):39–53.
37. Yamamoto T, Kudo M, Peng WX, Naito Z. Analysis of protein expression regulated by lumican in PANC1 cells using shotgun proteomics. Oncol Rep 2013;30(4):1609–1621.
38. Takaya A, Peng WX, Ishino K, Kudo M, Yamamoto T, Wada R, Takeshita T, Naito Z. Cystatin B as a potential diagnostic biomarker in ovarian clear cell carcinoma. Int J Oncol 2015;46(4):1573–1581.
39. Kanzaki A, Kudo M, Ansai S-I, Peng W-X, Ishino K, Yamamoto T, Wada R, Fujii T, Teduka K, Kawahara K, Kawamoto Y, Kitamura T, Kawana S, Saeki H, Naito Z, et al. Insulin-like growth factor 2 mRNA-binding protein-3 as a marker for distinguishing between cutaneous squamous cell carcinoma and keratoacanthoma. Int J Oncol 2016;48(3):1007–1015.
40. Yamamoto T, Kudo M, Peng W-X, Takata H, Takakura H, Teduka K, Fujii T, Mitamura K, Taga A, Uchida E, Naito Z, et al. Identification of aldolase A as a potential diagnostic biomarker for colorectal cancer based on proteomic analysis using formalin-fixed paraffin-embedded tissue. Tumour Biol 2016;37(10):13595–13606.
41. Takata H, Kudo M, Yamamoto T, Ueda J, Ishino K, Peng WX, Wada R, Taniai N, Yoshida H, Uchida E, et al. Increased expression of PDIA3 and its association with cancer cell proliferation and poor prognosis in hepatocellular carcinoma. Oncol Lett 2016;12(6):4896–4904.
42. Kawamura T, Nomura M, Tojo H, Fujii K, Hamasaki H, Mikami S, Bando Y, Kato H, Nishimura T. Proteomic analysis of laser-microdissected paraffin-embedded tissues: (1) stage-related protein candidates upon non-metastatic lung adenocarcinoma. J Proteomics 2010;73(6):1089–1099.
43. Zeisberg M, Neilson EG. Biomarkers for epithelial–mesenchymal transitions. J Clin Invest 2009;119(6):1429–1437.
44. Barrallo-Gimeno A, Nieto MA. The snail genes as inducers of cell movement and survival: Implications in development and cancer. Development 2005;132(14):3151–3161.
45. Shintani Y, Hollingsworth MA, Wheelock MJ, Johnson KR. Collagen I promotes metastasis in pancreatic cancer by activating c-Jun NH(2)-terminal kinase 1 and up-regulating N-cadherin expression. Cancer Res 2006;66(24):11745–11753.
46. Shintani Y, Wheelock MJ, Johnson KR. Phosphoinositide-3 kinase-Rac1-c-Jun NH2-terminal kinase signaling mediates collagen I-induced cell scattering and up-regulation of N-cadherin expression in mouse mammary epithelial cells. Mol Biol Cell 2006;17(7):2963–2975.
47. Koenig A, Mueller C, Hasel C, Adler G, Menke A. Collagen type I induces disruption of E-cadherin-mediated cell–cell contacts and promotes proliferation of pancreatic carcinoma cells. Cancer Res 2006;66(9):4662–4671.
48. Shintani Y, Maeda M, Chaika N, Johnson KR, Wheelock MJ. Collagen I promotes epithelial-to-mesenchymal transition in lung cancer cells via transforming growth factor-beta signaling. Am J Respir Cell Mol Biol 2008;38(1):95–104.
49. Hay ED. An overview of epithelio-mesenchymal transformation. Acta Anat (Basel) 1995;154(1):8–20.
50. Haensel D, Dai X. Epithelial-to-mesenchymal transition in cutaneous wound healing: Where we are and where we are heading. Dev Dyn 2017.
51. Chen L, Mai W, Chen M, Hu J, Zhuo Z, Lei X, Deng L, Liu J, Yao N, Huang M, Peng Y, Ye W, Zhang D, et al. Arenobufagin inhibits prostate cancer epithelial–mesenchymal transition and metastasis by down-regulating beta-catenin. Pharmacol Res 2017;123:130–142.